Experimental electron density and electrostatic potential analysis of zinc(aspirinate) 2 (H 2 O) 2 complex A 3d 10 metal bonding to a drug ligand

Anne Spasojevic - de Biré, N. Bouhmaida, A. Kremenović, G. Morgant, N.E. Ghermani

Experimental Electron Density and Electrostatic Potential Analysis of Zinc(Aspirinate)$_2$(H$_2$O)$_2$ Complex: a 3d^{10} Metal Bonding to a Drug-ligand.

Anne Spasojević-de Biré[†], Nouzha Bouhmaida[‡,*], Aleksandar Kremenović[†,£], Georges Morgant[§] and Nour Eddine Ghermani[$,†,*]

[†]*Laboratoire Structures, Propriétés et Modélisation des Solides (SPMS) UMR CNRS 8580, Ecole Centrale Paris, 1, Grande Voie des Vignes, 92295 Châtenay-Malabry cedex, France.*

[‡]*Laboratoire des Sciences des Matériaux, LSM, Université Cadi Ayyad, Faculté des Sciences Semlalia, Boulevard Prince Moulay Abdallah, BP 2390, 40000 Marrakech, Morocco.*

[§]*Laboratoire de Cristallographie Bio-inorganique, Université Paris XI, Faculté de Pharmacie, 5, Rue Jean-Baptiste Clément, 92296 Châtenay-Malabry cedex, France.*

[$]*Laboratoire de Physique Pharmaceutique UMR CNRS 8612, Université Paris XI, Faculté de Pharmacie, 5, Rue Jean-Baptiste Clément, 92296 Châtenay-Malabry cedex, France.*

[£]*permanent address : Department of Crystallography, Faculty of Mining and Geology, Djusina 7, 11000 Belgrade, Serbia, Yugoslavia.*

* Corresponding authors. Please address correspondence for any request to:
N. Bouhmaida Phone : +212 44 43 46 49, Fax : +212 44 43 74 10.
E-mail: nouzha@ucam.ac.ma
or N.E. Ghermani Phone : +33 (0)1 46 83 56 48, Fax : +33 (0)1 46 83 58 82.
E-mail: noureddine.ghermani@cep.u-psud.fr

Abstract

For the protection against the side effects and the improvement of the pharmacological activity of non-steroidal anti-inflammatory drugs (NSAID's), one alternative way is to design a metal complex of these agents. In this context, we have investigated the electrostatic properties of the zinc-aspirinate dihydrate ($Zn[C_9H_7O_4]_2(H_2O)_2$) complex in order to characterize and to mimic the activity of this potent pharmaceutical compound. A high resolution X-ray diffraction experiment at 100 K has been performed on the $Zn[C_9H_7O_4]_2(H_2O)_2$ complex which crystallizes in the *C2/c* space group displaying a tetrahedrally coordinated zinc atom. The Hansen-Coppens multipole model was used to derive the experimental electron density in order to study the chemical bonding and the metal-ligand charge transfer. The investigation of the electron density has revealed that only the Zn 4s orbital participates in the metal-ligand interaction whereas the metal 3d full valence shell remains unperturbated. The kappa-model refinement yielded a zinc net charge of +1.3 e with a highly contracted 4s electronic shell. The most positive charge of the aspirinate ligand was found on the acetyl carbon (+0.8 e) in agreement with the previously observed nucleophilic attack on the aspirin drug in the inhibited cyclooxygenase (COX) enzyme channel. The electrostatic potential was calculated from the multipole populations and the net atomic charges derived from the X-ray diffraction data. This fundamental property was carefully analyzed through the 3D isopotential and molecular surface representations in order to highlight the active sites of the zinc-aspirinate complex.

I. Introduction

Among the pharmaceutical anti-inflammatory agents, aspirin (acetylsalicylic acid) is the most used drug in a large domain of therapy. The aspirin interacts with the COX (cyclooxygenase) enzymes inhibiting the prostaglandin synthesis. Aspirin molecule displays two active sites: the COOH carboxylic acid and the acetyl group. The original feature of the aspirin interaction is the full transfer of the acetyl group of the molecule to the Ser-530 amino acid of the protein while the salicylic acid binds to Tyr-355 and Arg-120.[1-3] Non-steroidal anti-inflammatory drugs (NSAID's) like aspirin are well known to induce gastrointestinal complications and other important toxic effects related to the age and the physiological sensitivity of the patients. Also, a growing field of pharmacological investigations deals with the synthesis and biochemical characterizations of transition metal-based drugs. The activity of the drug ligand is often enhanced for such metal complexes[4]; this also permits to reduce the dose of the drug in the galenic formulation and to decrease the toxicity and the side effects of the parent active molecule. In addition, new activities of novel metal-based drugs can even arise like the anti-convulsant and anti-epileptic properties recently proven for copper salicylate complexes.[5]

The metal-based drug design generally involves transition metals. In addition, divalent ions like copper or zinc have their own biological activities in metalloenzymes and even display pharmaceutical properties (anti-viral). They also play a key role in the catalytic reactions *in vivo* or when the drug interacts with its enzymatic target. Chemically speaking, the transition metal properties are due to their ability to activate σ and π bonds involving ligand → metal donation and metal → ligand backdonation as reviewed by Boehme *et al.*[6] This is particularly true for the non-filled 3d subshell transition metal atoms like Fe, Co, Ni, and Cu for which the d-orbital electron occupancies generally conform to the crystal field theory with respect to their site coordination symmetries.[7] For Zn($3d^{10}4s^2$), the 3d shell is full and thus

energetically stable with respect to an acceptor ligand. The two electrons of the 4s orbital are expected to participate in the interaction and the charge transfer to the ligand, according to the formal +2 charge of the zinc metal. However, Weis *et al*.[8] have pointed out the influence of the $Zn^{+}(4s^{1})$ filled 3d orbital on a forced singly occupied 4s interacting with H_2 molecules in $Zn^{+}(H_2)_n$ clusters. From the experimental charge density study of $Zn(C_4O_4)(H_2O)_4$ metal squarate complexes[9] where the zinc is in an octahedral coordination, a metal net charge equal to 1.97 e and a 3d electron population of 8.40 e were reported. Other quantitative estimations of Zn charge (ranging from +0.7 to +1.7 e) were also found from DFT theoretical calculations in $[Zn(OH_n)]^{2-n}$ zincate complexes with respect to the metal-OH^{-} ligand distances and to the number of surrounding water molecules.[10] All these studies demonstrate how difficult can be the electronic structure description and bonding of the zinc metal atom. More recently, DFT calculations applied to Zinc-Methylimidazole[11] complex yield a charge donation in the range of 0.3-0.4 e from the anionic or neutral imidazole and water molecule ligands to the metal (net charge 1.6-1.7 e). This interesting study was carried out in order to illustrate and to mimic the metal interaction with the histidine residue in metalloenzymes. Comparatively, the aim of the electrostatic properties determination of a metal-drug complex can be twofold: the first objective is to characterize and to predict the reactivity of the complex considered as a chemical entity; the second one is to provide an insight into the interaction of the parent drug encountering metallic sites in the channel of the target enzyme. These goals are evidently of great interest for the understanding of drug-target interactions.

The present study deals with an experimental electrostatic properties investigation based on the low temperature (100 K) single-crystal high resolution X-ray diffraction applied to the Zn-aspirinate dihydrate ($Zn[C_9H_7O_4]_2(H_2O)_2$) compound (hereafter $Zn(Asp)_2(H_2O)_2$). The first crystallographic and solution ^{1}H NMR studies of $Zn(Asp)_2(H_2O)_2$ complex was reported by Hartmann and Vahrenkamp.[12] The authors have shown that the aspirinate remains

attached to Zn^{2+} ions in solution, which is an important result from a pharmaceutical point of view. In the solid state, Zn metal atom is tetrahedrally coordinated to two deprotanated aspirin molecules and two water molecules.[12] In the $Zn(Asp)_2(H_2O)_2$ compound, the aspirinate anion is a monodentate ligand involving only one oxygen atom of the COO^- carboxylate group. The previous crystal structure[12] was determined in the monoclinic *Cc* space group differentiating the molecular geometries of the two Zn-bonded aspirinate moieties with markedly high standard uncertainties (0.02 Å) in the reported atomic distances. The present low temperature high-resolution data permits to check the correct space group, which is found to be the monoclinic *C2/c* one. Diffraction data were refined using the multipole electron density Hansen-Coppens model.[13] The results of the experimental electron density and the derived electrostatic potential are presented in order to show up the Zn-ligand bonding features and to locate the electrophile/nucleophile regions around this potent pharmaceutical metal complex of aspirin. The atomic net charges are also estimated in order to quantify the metal-ligand electron transfer of the aspirin complex. Finally, the electrostatic potential is carefully analysed on the complex surface and used as a predictive tool for further interactions.

II. Experimental and Methods

1. Data collection. A suitable sample of a $Zn(Asp)_2(H_2O)_2$ colorless crystal with dimensions 0.34 x 0.32 x 0.32 mm was used for the high resolution X-ray diffraction experiment. The data were collected at 100.0(1) K on a Bruker-SMART three axis diffractometer equipped with a SMART 1000 CCD area detector using graphite monochromated MoKα X-radiation (wavelength λ = 0.71073 Å). The low temperature was reached by an evaporated liquid nitrogen flux over the crystal, provided by the Oxford Cryosystem device. The area detector surface was placed at 5 cm from the crystal sample. The diffraction data were collected at six different detector positions: 2θ = 0, ±28, ±68, 85° where

θ is the Bragg angle. The data spots were recorded as ω-scans (Δω = 0.15°) in order to reconstruct accurate three dimensional diffracted intensity profiles. According to the θ-dependence of the diffracted intensities, the chosen exposure times were 10, 25, 40 and 45 seconds for the detector positions at 2θ = 0, ±28, ±68, 85°, respectively. The maximum resolution reached for this experimental data set is $(\sin\theta/\lambda)_{max}$ = H/2 = 1.15 $Å^{-1}$, where H is the Bragg vector modulus. 74648 symmetry-equivalent and redundant measurements were collected in this experiment. The Lorentz-polarization correction and the integration of the diffracted intensities were performed with the SAINT software package.[14] The orientation matrix was optimized every 100 frames during the intensity integration processing. The final refined cell parameters are given in Table 1. An empirical absorption correction was applied using the SADABS[14] computer program. For this procedure, 40747 high-intensity reflections (I/σ(I) ≥ 5.0, σ(I) being the estimated standard deviation of the intensity I) have been employed. Finally, the SORTAV[15] program was used for sorting and averaging data in 2/m point group giving a total of 10807 unique reflections and a final internal factor R_{int} = 3.0 %. 5056 unique reflections (I>3σ(I)) were used in the conventional and electron density refinements. Details of the X-ray diffraction experiment conditions and the crystallographic data for the $Zn(Asp)_2(H_2O)_2$ compound are given in Table 1.

2. Electron density distribution. In the Hansen-Coppens model[13] we used, the molecular electron density is the sum of pseudo-atomic contributions expressed as

$$\rho_{at}(\mathbf{r}) = \rho_{\text{core}}(\mathbf{r}) + P_{\text{val}}\kappa^3\rho_{\text{val}}(\kappa\mathbf{r}) + \kappa'^3\sum_{l=0}^{l\max} R_{\text{nl}}(\kappa'\mathbf{r})\sum_{m=0}^{l} P_{\text{lm}\pm}\, y_{\text{lm}\pm}(\theta,\varphi) \qquad (1)$$

where $\rho_{core}(r)$, $\rho_{val}(r)$ describe the frozen core and valence spherical densities both obtained from the Hartree-Fock wave functions of the free atoms or ions.[16] κ is a contraction–expansion coefficient of the spherical valence electron density and P_{val}, the corresponding refined electron population. Therefore, the atomic charge can be estimated as

$q = P_{val} - N_{val}$ where N_{val} is the valence population of the free atom or ion. The aspherical part of the pseudo-atom electron density is projected onto a real normalized harmonics $y_{lm\pm}$ basis set (l = 0 (monopole) to 4 (hexadecapole)) and modulated by a Slater-type radial function $R_{nl}(r) = Nr^{n_l} \exp(-\xi_l r)$, where N is the normalization factor. In equation (1), κ' is a contraction-expansion coefficient used to adjust the maximum of the radial function and $P_{lm\pm}$ are the multipole populations of the pseudo-atom electron deformation density. The ξ_l exponents[17] (in $bohr^{-1}$) are chosen equal to 3.0, 4.5 and n_l = 2, 2, 3 up to octupoles (l = 3) for C and O atoms respectively; ξ_l = 2.26 $bohr^{-1}$ and n_l = 1 (dipole level, l = 1) for the hydrogen atoms. Assuming that the 3d shell electron density of a transition metal like $Zn(3d^{10}4s^2)$ is fully described by the even orders[18-19] l = 0, 2, 4 of the multipolar expansion (equation 1), one monopole (P_{00}), the quadrupoles and hexadecapoles can be introduced for the zinc. For all refinements in this study, the P_{val} population was always assigned to the more diffuse 4s electron density of the zinc metal atom.

3. Refinement strategies. Based on the high-resolution low temperature data, the crystal structure determination and conventional refinements were first carried out using the WINGX software package.[20] The careful examinations of the atomic distances and geometries of the symmetrically equivalent molecules confirm the centrosymmetric *C2/c* space group for $Zn(Asp)_2(H_2O)_2$ in the solid state. The previous room temperature structure of this complex was, however, reported in the *Cc* space group with a less accuracy and an evident correlation of the atomic bond lengths.[12] Conventional and electron density refinements were then carried out using the MOLLY[13] program with the full matrix least-squares procedure minimizing the error function $\Delta = \sum w_H (K^{-1}|F_o| - |F_c|)^2$, where K is the scale factor, $w_H = 1/\sigma_H^2$ is the statistical weight (σ^2_H being the variance of the diffracted intensity at **H** Bragg vector) and

F_o, F_c are the observed and calculated structure factors, respectively. Atomic coordinates and anisotropic thermal displacement amplitudes were first estimated by the fit to high-order data ($\sin\theta/\lambda \geq 0.8$ Å^{-1}) for non-H atoms before the electron density refinements. An isotropic thermal motion was assumed to H atoms positioned using all diffraction data. Residual Fourier maps calculated with high-order data have revealed the features of an anharmonic thermal motion of Zn. Therefore, the Gram-Charlier expansion up to the 6th order[21] was introduced for the metal atom in our refinements.

The numbering scheme of the $Zn(Asp)_2(H_2O)_2$ complex is depicted in Figure 1. In order to reduce the number of the refined parameters and to avoid their unrealistic shifts during the least-squares procedure, the atomic chemical equivalence has been employed. Accordingly, during the electron density refinements, chemical constraints were applied to the phenyl carbons $C_3 = C_4 = C_5 = C_6$, to their corresponding hydrogen atoms $H_3 = H_4 = H_5 = H_6$, and to those of C_9 methyl $H_{91} = H_{92} = H_{93}$ as well. For the water molecule, we also consider $H_{w1} = H_{w2}$ in the electron density model description for the sake of stability in the least-squares fit. Before the electron density refinement procedure, the positions of the hydrogen atoms were extended to their neutron corresponding distances ($C_{aromatic}$-H = 1.08 Å, C_{methyl}-H = 1.07 Å and O_{water}-H = 0.96 Å). These bond lengths were relaxed in the last cycles of the refinements. In addition, H valence κ-parameters (equation 1) were held fixed at 1.16 corresponding to bonded hydrogen atoms in the C-H and O-H links.

The multipole refinements were started by considering a neutral zinc atom with separated 3d and 4s valence shells. The valence electron populations were attributed to the refined monopoles $P_{val}(4s)$ and $P_{00}(3d)$ respectively. The hybridization of the 3d and 4s valence shells gave unstable refinement results and was excluded. Moreover, all attempts to refine the Zn multipole parameters failed and have yielded unrealistic 3d occupations significantly larger than 2 electrons per orbital. The second monopole $P_{00}(3d)$ refined value

remained stable at 10 e and was fixed in the subsequent refinements. Consequently, only the Zn 4s orbital interaction with the ligands has been finally considered in this study. In the multipole refinements, an electroneutrality constraint was imposed either on the whole system (metal + the two ligands) or on Zn-aspirinate on the one hand and the water molecule on the other. Therefore, the charge transfer between the metal and the separate ligands has been estimated. The statistical least-squares factors did not significantly change for these two strategies. The common final R residual factors and the goodness-of-fit (gof) close to 1.0 attesting the good convergence of the multipole refinement are given in Table 1.

4. Electrostatic properties. A multipole fit to low temperature high resolution X-ray data generally permits the best decorrelation between the atomic electron density and the thermal motion contributions to the observed structure amplitudes. After a multipolar refinement, the atomic positions and thermal parameters recover their best estimate and accuracy. The experimental net atomic charges determination can then be carried out using the κ-refinement[22] involving the spherical part in equation 1. This model is mainly useful to explore the charge transfer and the electron repartition inside the molecule or between a donor and an acceptor chemical system.

The full set of the refined atomic electron density parameters can be directly used to retrieve electrostatic properties for a molecule at rest and isolated from the crystal. For this purpose, we have developed a software package[23] in order to calculate the electrostatic properties derived from the multipole model parameters. The computer programs were extended to transition metal atoms like zinc in this study. The molecular bond features (single or double bond, lone pairs, polarization etc…) can simply be analysed through the examination of the static electron deformation density calculated as the difference between pseudo-atom and Hartree-Fock[16] free-atom electron densities (promolecule). A deeper characterization necessitates, however, a topological study of the electron density. In the

present work, we focused on the electrostatic potential as a guide to the molecular reactivity and as a predictive tool for further recognition between drugs and receptors. The electrostatic potential remains the main property to investigate the nucleophilic/electrophilic interaction zones around a given molecule. Our programs[23] have been recently modified to calculate and display the useful experimental 3D isovalue potential[24] and the electrostatic potential on particular molecular surfaces defined below.

III. Results and discussion

1. Molecular structure and crystal packing. $Zn(Asp)_2(H_2O)_2$ crystallizes in the *C2/c* space group with the Zn transition metal located on the twofold symmetry-axis. Figure 2 depicts the ORTEP[20,25] view of the $Zn(Asp)_2(H_2O)_2$ complex in the solid state. The zinc atom has a distorted tetrahedral coordination with two carboxylate O_1 oxygen atoms and two O_w water-ligand ones. In the crystal structure, the metal positions form a zig-zag line parallel to the **c**-crystallographic axis. In this direction, two adjacent $Zn(Asp)_2(H_2O)_2$ units have opposite orientations. To reduce the steric hindrance, Zn-aspirinate complexes are much more separated along the **a** unit cell axis (a = 25.219(3) Å). This gives rise to a molecular arrangement where the phenyl groups of the aspirinate anions are almost in parallel planes. The main bond lengths and angles calculated after the multipole refinement are listed in Table 2. The values obtained are not in agreement with those reported in the room temperature study[12] especially for the organic part of the complex. In the present research, Zn-O_1 and Zn-O_w bond distances are equal to 1.9957(5) Å and 2.0190(4) Å respectively, thus significantly different with respect to the estimated standard deviations. In the $Zn(Asp)_2(H_2O)_2$ crystal**,** the aspirinate anion acts as a monodentate ligand since the Zn-O_2 distance equals 2.5200(5) Å. The smallest angle is O_w–Zn–O_w = 91.76(3)° whereas the largest one occurs between the carboxylate oxygen atoms O_1–Zn–O_1 = 135.34(3)°, mainly

due to the steric and repulsive effects between aspirinate anion ligands. As observed in the crystal structure of aspirin[26] and also retrieved from the theoretical *ab initio* structural optimization[27], the phenyl acetate exhibits an *s*-trans conformation where the dipole of the ester group is oriented towards the phenyl ring. In the present study, the COO^- plane of the ester is almost perpendicular to that of the phenyl ring (dihedral angle $C_8{-}O_3{-}C_7{-}C_6$ = 119.42(7)°). On the other hand, the carboxylate group is not coplanar with the phenyl ring as also reported for the isolated aspirin molecule[26,27], the corresponding dihedral angle found in the crystal is $O_2{-}C_1{-}C_2{-}C_3$ = –32.32(8)°. The $C_1{-}O_1$ and $C_1{-}O_2$ bond distances are 1.279(1) Å and 1.251(1) Å, respectively. Comparatively, in the ester group, the bond distances are much different: $C_8{-}O_3$ = 1.359(1) Å and $C_8{-}O_4$ = 1.208(1) Å. The crystal packing of $Zn(Asp)_2(H_2O)_2$ exhibits two intermolecular hydrogen bonds: both the ester carbonyl oxygen O_4 and the carboxyl oxygen O_2 are hydrogen bond acceptors. They strongly bind to H_{w1} and H_{w2} hydrogen atoms of the water molecule ($O_2{---}O_w$ = 2.6555(6) Å, $O_2{-}H_{w2}{-}O_w$ = 173.83(3)°; $O_4{---}O_w$ = 2.7698(6) Å, $O_4{-}H_{w1}{-}O_w$ = 172.69(4)°).

2. Electron density maps. The multipole refinements with constrained and unconstrained electroneutrality of the water molecule gave similar trends of the electron density around the $Zn(Asp)_2(H_2O)_2$ complex. The maps presented in this section correspond to those obtained from the multipole refinement with an electroneutrally refined H_2O molecule. The residual electron densities are computed as a Fourier transform of the $\left(F_o - F_c\right)$difference, where F_o and F_c are the observed and model calculated structure factors respectively. The residual electron density maps permit to localize the electron density peaks unfitted by the used model. In this study, the Fourier summation was performed over all the data in order to judge the quality of the full set of observations. Residual electron density maps in the planes of the carboxylate ($O_1{-}C_1{-}O_2$) and the acetyl group ($O_3{-}C_8{-}O_4$) are

presented in Figure 3 (a and b respectively). In Figure 3a the Zn atom is at 0.12 Å from the plane of the carboxylate group. The residual maps are featureless apart from the residue of 0.4 $eÅ^{-3}$ due to the low order data (valence contribution) and found at approximately 1 Å from the zinc atom site (Figure 3a). As pointed out in the previous section, attempts to reduce or to interpret these residues by including the multipole refinements of the Zn 3d electronic shell failed and led to unrealistic values of orbital occupations. The introduction of the hybridization of the Zn 4s and 3d shells has neither improved our model.

The static electron deformation density was calculated as the difference between the model and the Hartree-fock free atom densities using our STATDENS program.[23] Figure 4 (a and b) depicts the static electron deformation density in the carboxylate and the acetyl group planes respectively. In the plane of the carboxylate group (Figure 4a), the contraction of the zinc 4s electronic shell can be shown since the metal is not completely ionised; a zinc charge equal to +1.0 e (P_{val} = 1.00(2) and 0.96(3) for the neutral and free water molecule strategies respectively) was obtained in the multipole refinements. This contraction is in agreement with the Pauli repulsion between the metal and ligand electron clouds. In the carboxylate group (Figure 4a), the O_1 oxygen atom lone pair charge density is clearly polarized towards the Zn atom. On the other hand, similar trends of C–O bonds in the two chemical groups (carboxylate and acetyl) are shown in both maps in Figure 4 despite of the quite differences in the bond lengths (see Table 2). For the two groups, the C–O bond electron deformation density peak heights vary from 0.5 to 0.6 $e/Å^3$. An exception can, however, be made for the C_7–O_3 (1.396(1) Å) bond electron deformation density which does not exceed 0.2 $e/Å^3$. Especially for the O_3–C_8–O_4 fragment, bond distances and equivalent electron densities in C_8–O_3 and C_8–O_4 bonds are found to conform to the well-known ester resonance. If the O_3 lone pairs respect a regular sp^3 electron configuration, O_4 ones are markedly

distorted and one lone pair is preferentially oriented towards the close hydrogen bonded water molecule as shown in Figure 4b, the other lone pair being out of the plane of this figure.

3. Net atomic charges. The net atomic charges in the $Zn(Asp)_2(H_2O)_2$ complex have been estimated from the κ-model[22] refinements. In this work, we remember that only the Zn 4s valence orbital population has been introduced in the metal-ligand interaction. The results are presented in Table 3 for the neutral and free charged water ligand. The κ-refinement yielded a zinc charge of +1.3 e (+1.2 e for free charged water molecule) with a highly contracted 4s electronic shell (κ = 1.8(1)). The metal donation locally involves the carboxylate oxygen atoms with charges close to –0.6 e. In the unconstrained refinement (Table 3), the water molecule became slightly positive (+0.13(5) e) due to a less negatively charged oxygen atom. From the two refinements, the total charge of the aspirinate ligand is found to be in the narrow range of 0.65 e (neutral H_2O) to 0.75 e (free H_2O). We can also emphasize that the charge repartition trends in the organic part of the complex are quantitatively similar from the two strategies of fit within the estimated error intervals. It is worthnoting, however, that the two κ-refinements reveal high values of atomic charges for the ester group. Indeed, the most positive charge equal to +0.8 e has been obtained for C_8 atom compared to +0.6 e found for the corresponding C_1 carboxylate carbon. The most negative charge is that of the C_9 methyl carbon (–0.7 e). These results confirm the high electrophilicity of the C_8 carbon atom of the acetyl group displaying a polar character. Therefore, a nucleophilic attack can be expected at this carbon site of the zinc complex of aspirin. This is in agreement with the recent study on the interaction of the isolated aspirin with COX-2 cyclooxygenase isomer which has shown that the acetylation of the Ser-385 amino acid involves the corresponding ester carbon atom.[2] From these solid state results and with the hypothesis that the molecular conformation does significantly not change in the enzyme channel, we can conclude that the esterase activity remains possible for the zinc complex of

aspirin. This probably would be more problematic for the dimetallic copper-aspirinate complex[28] where the corresponding O_4 ester oxygen is bounded to the metal atom (Cu–O = 2.241(8) Å).

4. Electrostatic potential analysis. A very useful way to investigate the electrostatic potential features is the use of the 3D isosurface representation since it gives the quantification of the extent of this fundamental property around the chemical systems. However, if such isosurfaces well illustrate the long-range character of the electrostatic potential especially for isolated molecules, they do not closely reflect the interaction in condensed phases. For this reason, another complementary and helpful approach to understand the non-covalent interactions was developed on the basis of the inspection of the electrostatic potential variations on particular molecular surfaces. The availability of the visualization freeware programs like MOLMOL[29] has made these two representations easily accessible to our 3D computed values of the electrostatic potential.

Figure 5 displays the electrostatic potential generated around the isolated $Zn(Asp)_2(H_2O)_2$ complex using the refined multipole (Figure 5a) and κ-model parameters (Figure 5b) respectively. The isopotential surfaces drawn in these figures correspond to –0.1 and + 0.2 e/Å (1e/Å = 332.4 kcal/mol). It is worthwhile to note that the isolated complex displays an electrostatic potential with a polar character. This is more visible in Figure 5b showing the contribution of the net atomic charges obtained from the κ-refinements. The crystal packing described in the previous section certainly obeys to an anti-parallel arrangement of dipolar $Zn(Asp)_2(H_2O)_2$ units. The positive potential barycentre is located approximately on the zinc site whereas the negative one is in the interior of the angle formed by the two aspirinate ligands. As expected, the negative potential is reduced due to the positive contribution of the metal partially inhibiting the nucleophilic regions around the carboxylate groups and the water molecules. Nevertheless, an extended negative electrostatic

potential surrounds all oxygen atoms of the organic ligands in Figure 5a obtained from the multipole parameters. This is not true for the κ-model electrostatic potential shown in Figure 5b where the nucleophilic zone is contracted between the aspirinate ligands. Conversely, the electrophilic region around $Zn(H_2O)_2$ and the phenyl groups of the complex is more expanded. The trends observed for the net charges generated electrostatic potential are well known due to the fact that only the multipole parameters are able to reflect π or lone pair contributions in the vicinity of a chemical system.

In order to use the electrostatic potential as a predictive tool for non-covalent interactions, we have performed molecular surface calculations for the $Zn(Asp)_2(H_2O)_2$ complex isolated from the crystal. Many definitions of molecular surfaces can be found in literature especially for large molecules like proteins: Connolly, van-der-Waals, solvent accessible surface etc… From the quantum mechanics theory, the concept of the molecular surface has been accurately discussed by Bader *et al*.[30] Based on the same idea, the research group of Murray and Politzer[31,32] has extensively used the 0.001 au (≈ 0.007 e/Å^3) isodensity surface to define the molecular envelop. The surface electrostatic potential statistical variance was considered by these authors as a quantitative index to retrieve macroscopic properties in different phases of matter (gaz, liquid, solid).[33,34,35] In the present study, the refined multipole parameters were utilized to compute the molecular surface (ρ = 0.007 e/Å^3) potential of the $Zn(Asp)_2(H_2O)_2$ complex. The results obtained with the net charges from the κ-refinements do not change the qualitative conclusions given below. Figure 6 depicts the isodensity surface colored by the multipolar electrostatic potential in the range of magnitude corresponding to ± 0.2 e/Å. There are many localized centers of negative (red) and positive (blue) electrostatic potential mainly associated with the acetyl and carboxylate oxygen atoms on the one hand, and the water and phenyl hydrogen atoms on the other. The zinc positive contribution to the electrostatic potential does not appear on the external surface of the complex. However, the

peripheral surface potential is electrophilic around the phenyl rings wheareas the most nucleophilic region is in the confined cavity formed by the close acetyl groups (Figure 6b) of the aspirinate ligands. Figures 6b also shows that the acetyl group is accessible from the outside with a slight concave electron density surface presented by the C_8 carbon atom. Furthermore, we note in Figure 6c that around the C_8 ester carbon site, the electrostatic potential varies in sign and magnitude due to the close proximity of oxygen (O_3, O_4) and hydrogen atoms (methyl, phenyl). These atoms can play a role of anchors for an approaching molecule due to their respective strong positive and negative electrostatic potential contributions.

IV. Summary and Conclusion

The accurate molecular structure and the electron density of the $Zn(Asp)_2(H_2O)_2$ complex were derived from a 100 K high resolution X-ray diffraction experiment. The zinc is tetrahedrally coordinated to two monodentate aspirinate anions involving their carboxylate groups and to two water molecule ligands. Electron density peaks were observed in the vicinity of the zinc site but they could not be interpreted in terms of a Zn 3d orbital instability. Therefore, only the Zn 4s valence shell has been taken into account in the electron density multipole model in order to explore the metal-ligand bonding. κ-model refinements were carried out to estimate the net atomic charges and the metal-ligand electron transfer. It has been shown that the zinc net charge is +1.3 e in the $Zn(Asp)_2(H_2O)_2$ compound demonstrating that the metal-aspirinate interaction has not completely an ionic character. The activity of the zinc-aspirinate complex was revealed for the acetyl group of the drug ligand. From the atomic charge obtained for the ester carbon (+0.8 e), we were able to conclude, that the esterase remains highly probable for the aspirin ligand in the zinc complex.

Both the isovalue and molecular surface electrostatic potential representations were used in this study. These allow us to localize the active sites around the zinc complex of

aspirin. The interactions in a biological medium are obviously different and both the molecular conformation and electronic polarization can be modified with respect to the chemical environment. A comparison between experiment and theoretical calculations would permit to go further in the interpretation of the pharmaceutical potency of the zinc-aspirinate complex.

Acknowledgments

The financial support of the CNRS, Ecole Centrale Paris, Université de Paris XI, Université Cadi Ayyad and University of Belgrade is gratefully acknowledged. The authors would like to thank Pr B. Viossat for providing crystal samples of $Zn(Asp)_2(H_2O)_2$ and Pr N.K. Hansen for the fruitful discussions and advises on this work.

Supporting Information Available: Fractional coordinates and atomic thermal parameters (Sup I); Significant Gram-Charlier coefficients and their estimated standard deviations (esd's) for anharmonic thermal vibration of Zn (Sup II); κ, κ', P_{val} and P_{lm} multipole parameters for $Zn(Asp)_2(H_2O)_2$ (Sup III).

References

(1) Loll, P.J.; Picot, D.; Garavito, R.M. *Nat. Struct. Biol.* **1995**, *2*, 637.

(2) Hochgesang Jr., G. P.; Rowlinson, S.W.; Marnett, L.J. *J. Am. Chem. Soc.* **2000**, *122*, 6514.

(3) Glaser, R. *J. Org. Chem.* **2001**, *66*, 771.

(4) Sorenson, J.R.J. in *Handbook of Metal-Ligand Interactions in Biological Fluids: Bioinorganic Medicine,* G. Berthon Editor, **1995**, *2*, M. Dekker, New York.

(5) Lemoine, P.; Viossat, B.; Morgant, G.; Greenaway, F.T.; Tomas, A.; Nguyen-Huy, D.; Sorenson, J.R.J. *J. Inorg. Biochem.* **2002**, *89*, 1-2, 18.

(6) Boehme, C.; Uddin, J.; Frenking, G. *Coord. Chem. Rev.* **2000**, *197*, *1*, 249.

(7) Koritsanszky, T.S.; Coppens, P. *Chem. Rev*. **2001**, *101*, 1583.

(8) Weis, P.; Kemper, P.R.; Bowers, M.T. *J. Phys. Chem.* **1997**, *101*, 2809.

(9) Lee, C. ; Wang, C.; Chen, K.; Lee, G.; Wang, Y. *J. Phys. Chem. A* **1999**, *103*, 156.

(10) Smith, G. D.; Bell, R.; Borodin, O.; Jaffe, R.L. *J. Phys. Chem. A* **2001**, *105*, 6506.

(11) Hasegawa, K.; Ono, T.; Noguchi, T. *J. Phys. Chem. A* **2002**, *106*, 3377.

(12) Hartmann, U.; Vahrenkamp, H. *Bulletin of the Polish Academy of Sciences, Chemistry* **1994**, *42*, *2*, 161.

(13) Hansen, N.K.; Coppens, P. *Acta Crystallogr.* **1978**, *A34*, 909.

(14) *ASTRO (5.007), SAINT (5.007) and SADABS (5.007). Data Collection and Processing Software for the SMART System (5.054).* Siemens (BRUKER-AXS) Analytical X-ray Instruments Inc. **1998**, Madison, Wisconsin, USA.

(15) Blessing, R.H. *J. Appl. Crystallogr.* **1997**, *30*, 421.

(16) Clementi, E.; Roetti, C. *Atomic data and Nuclear data tables*. Academic press, New York, USA, **1974**, *14*, 177.

(17) Clementi, E. ; Raimondi, D.L. *J. Chem. Phys.* **1963**, *41*, 2686.

(18) Stevens, E.D., Coppens, P. *Acta Crystallogr.* **1979**, *A35*, 536.

(19) Holladay, A., Leung, P., Coppens, P. *Acta Crystallogr.* **1983**, *A39*, 377.

(20) Farrugia, L.J. *J. Appl. Crystallogr.* **1999**, *32*, 837.

(21) Kuhs, W.F. *Acta Crystallogr.* **1983**, *A39*, 148.

(22) Coppens, P.; Guru, T.N.; Leung, P.; Stevens, E.D.; Becker, P.; Yang, Y.W. *Acta Crystallogr.* **1979**, *A35*, 63.

(23) Ghermani, N.E.; Bouhmaida, N.; Lecomte, C. ELECTROS, STATDENS, FIELD+: *Computer programs to calculate electrostatic properties from high resolution X-ray diffraction.* **1992-2001**. Internal report UMR CNRS 7036, Université Henri Poincaré, Nancy 1, France ; UMR CNRS 8612, Université Paris XI, France and Université Cadi Ayyad, Morocco.

(24) Bouhmaida, N.; Dutheil, M. ; Ghermani, N.E. ; Becker, P. *J. Chem. Phys.* **2002**, *116*, *14*, 6196.

(25) Burnett, M.N.; Johnson, C. K. ORTEP-III report ORNL-6895, **1996**, Oak Ridge International Laboratory, Tennessee, USA.

(26) Meenan, P. *ACS Symp. Ser*., **1997**, *667*, 2.

(27) Glaser, R. *J. Org. Chem.* **2001**, *66*, 771.

(28) Manojlovic-Muir, L. *Acta Crystallogr.* **1973**, *B29*, 2033.

(29) Koradi, R.; Billeter, M.; Wüthrich, K. MOLMOL: *a program for display and analysis of macromolecular structures. J. Mol. Graphics* **1996**, *14*, 51.

(30) Bader, R.F.W.; Caroll, M.T.; Cheeseman, J.R.; Chang, C. *J. Am. Chem*. Soc. **1987**, *109*, 7968.

(31) Murray, J.S.; Politzer, P. *J. Chem. Res.* **1992**, S, 110.

(32) Brinck, T.; Murray, J.S.; Politzer, P. *Mol. Phys*. **1992**, *76*, 609.

(33) Murray, J.S.; Brinck, T.; Politzer, P. *Chem. Phys.* **1996**, *204*, 289.

(34) Murray, J.S.; Politzer, P. *J. Mol. Struc*. **1998**, *425*, 107.

(35) Politzer, P.; Murray, J.S. *Fluid Phase Equilibria* **2001**, *185*, 129.

List of Tables

TABLE 1: Crystallographic data and experimental details of $Zn(Asp)_2(H_2O)_2$.

Formula	$Zn[C_9H_7O_4]_2(H_2O)_2$
Formula weight	459.7
Crystal system	Monoclinic
Space group	C 2/c
Crystal size, color	0.34 x 0.32 x 0.32 mm, colorless
a	25.219(3) Å
b	7.101(1) Å
c	11.125(1) Å
α	90°
β	108.353(7)°
γ	90°
Z	4
Volume	1890.8(5) $Å^3$
Density	1.61 g cm^{-3}
μ	1.35 mm^{-3}
T	100.0(1) K
λ	0.71073 Å
$(\sin\theta/\lambda)_{max}$	1.15 $Å^{-1}$
Reflections collected	74648
Unique reflections	10807
Reflections used [I>3σ(I)]	5056
R_{int}	3.0 %
Multipole refinement	
R[F]	1.89%
R_w[F]	1.72%
g.o.f	0.99

Statistical factors are defined as:

$R_{\text{int}} = \frac{\sum(I - \langle I \rangle)}{\sum I}$ I is the Bragg intensity

$$R[F] = \frac{\sum(K^{-1}|F_o| - |F_c|)}{\sum K^{-1}|F_o|}, \quad R_w[F] = \left[\frac{\sum w(K^{-1}|F_o| - |F_c|)^2}{\sum wK^{-2}|F_o|^2}\right]^{\frac{1}{2}} \quad g.o.f = \left[\frac{\sum w(K^{-1}|F_o| - |F_c|)^2}{m-n}\right]^{\frac{1}{2}}$$

$|F_o|$ and $|F_c|$ are the moduli of the observed and the calculated structure factor respectively, K is the scale factor, *w* the statistical weight, *n* is the number of refined parameters and *m* the number of used data.

TABLE 2: Bond lengths (Å) and selected angles (°) of $Zn(Asp)_2(H_2O)_2$. Estimated standard deviations are given in parentheses.

$Zn-O_1$	1.9957(5)	O_1-Zn-O_1''	135.34(3)
$Zn-O_w$	2.0190(4)	O_w-Zn-O_w''	91.76(3)
$Zn-O_2$	2.5200(5)	O_1-Zn-O_w	112.02(2)
C_1-O_1	1.279(1)	O_1-Zn-O_w''	98.85(2)
C_1-O_2	1.251(1)		
C_7-O_3	1.396(1)		
C_8-O_3	1.359(1)		
C_8-O_4	1.208(1)		
C_1-C_2	1.500(1)	$O_1-C_1-O_2$	121.35(5)
C_2-C_3	1.402(1)	$O_3-C_8-O_4$	122.12(5)
C_2-C_7	1.402(1)	$C_7-O_3-C_8$	117.95(5)
C_3-C_4	1.395(1)		
C_4-C_5	1.395(1)		
C_5-C_6	1.397(1)		
C_6-C_7	1.389(1)		
C_8-C_9	1.491(1)		

$''$symmetry operation: -x, y, 3/2-z

TABLE 3: Atomic net charges (in e) of $Zn(Asp)_2(H_2O)_2$. Estimated standard deviations are given in parentheses for refined parameters.

	neutral H_2O		free H_2O	
	κ	charge	κ	charge
Zn	1.8(1)	+1.29(4)	1.7(1)	+1.24(4)
C_1	1.06(1)	+0.60(6)	1.06(1)	+0.62(6)
O_1	0.964(4)	-0.59(4)	0.966(4)	-0.58(4)
O_2	0.965(4)	-0.53(4)	0.970(4)	-0.50(4)
C_2	1.03(1)	-0.16(6)	1.03(1)	-0.18(6)
C_3=C_4=C_5=C_6	1.041(4)	-0.06(2)	1.039(4)	-0.08(2)
H_3=H_4=H_5=H_6	1.16	+0.06(1)	1.16	+0.05(1)
C_7	1.07(1)	+0.25(6)	1.07(1)	+0.25(6)
C_8	1.09(1)	+0.82(6)	1.09(1)	+0.79(6)
O_3	0.986(4)	-0.45(4)	0.987(4)	-0.45(4)
O_4	0.967(4)	-0.40(4)	0.969(4)	-0.39(4)
C_9	0.987(8)	-0.73(9)	0.987(8)	-0.74(9)
H_{91}=H_{92}=H_{93}	1.16	+0.17(2)	1.16	+0.18(2)
O_W	0.963(4)	-0.63(4)	0.971(4)	-0.55(4)
H_{W1}=H_{W2}	1.16	+0.32(2)	1.16	+0.34(2)

Figure Captions

Figure 1 : Numbering scheme of $Zn(Asp)_2 (H_2O)_2$.

Figure 2 : ORTEP view of the $Zn(Asp)_2 (H_2O)_2$ compound.

Figure 3 : Residual electron density maps : a) C1–O1–O2 plane, b) C3–O4–O3 plane. Contours interval is 0.1 $eÅ^{-3}$; negative contours are dashed, zero contour omitted.

Figure 4 : Static electron deformation density maps : a) C1-O1-O2 plane, b) C3-O4-O3 plane. Contours are as in figure 3.

Figure 5 : Isopotential surfaces around $Zn(Asp)_2 (H_2O)_2$ complex. Yellow and red surfaces correspond to +0.20 $eÅ^{-1}$ and –0.10 $eÅ^{-1}$ respectively. a) From multipole refinements.
b) From the kappa-refinement.

Figure 6 : Isodensity (0.007 $eÅ^{-3}$) molecular surface colored by the electrostatic potentiel generated around $Zn(Asp)_2 (H_2O)_2$ complex. Blue and red colours correspond to +0.20 $eÅ^{-1}$ and –0.20 $eÅ^{-1}$ respectively. a) view from the top. b) and c) around the acetyl group.

Figure 1

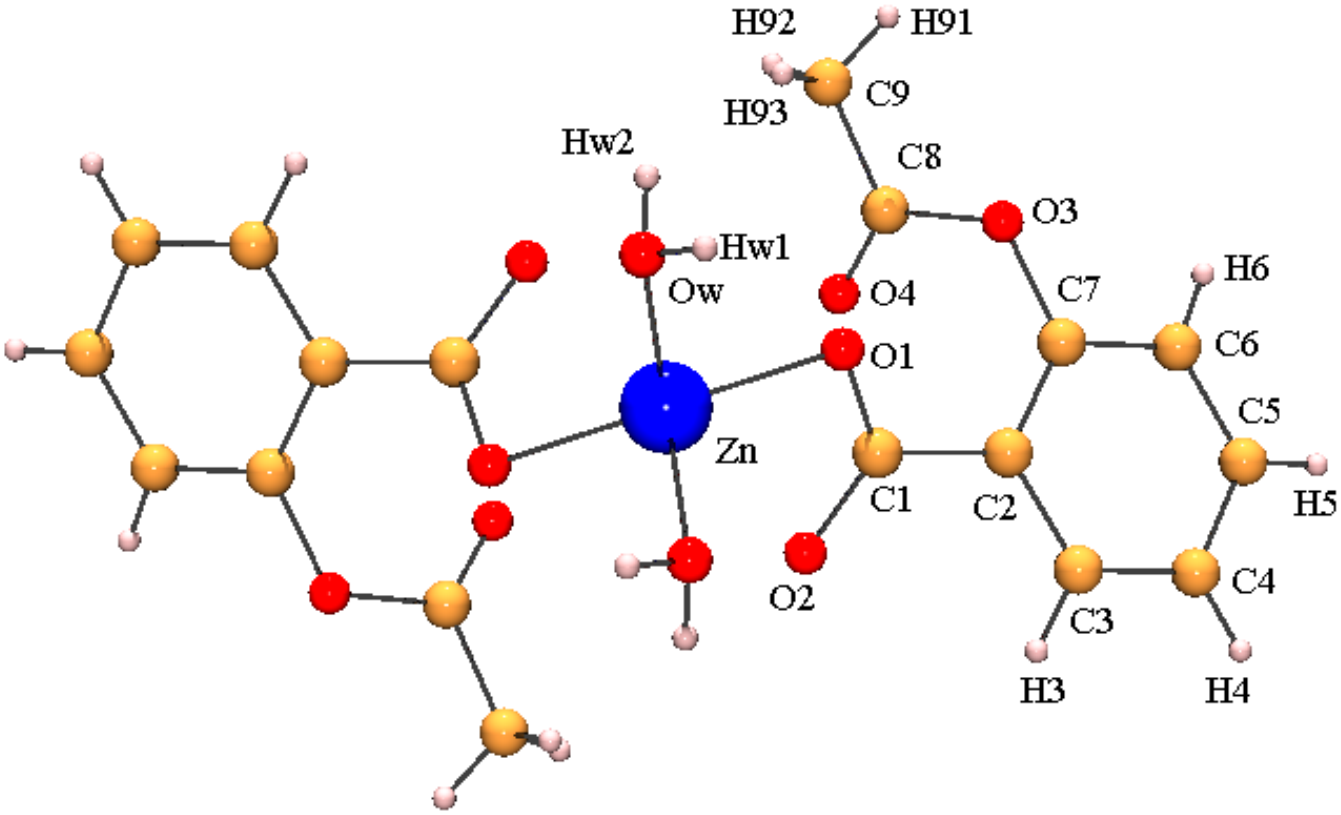
H92
H91
C9
H93
Hw2
C8
O3
Hw1
Ow
O4
C7
H6
O1
C6
C5
Zn
C1
C2
H5
O2
C4
C3
H3
H4

Figure 2

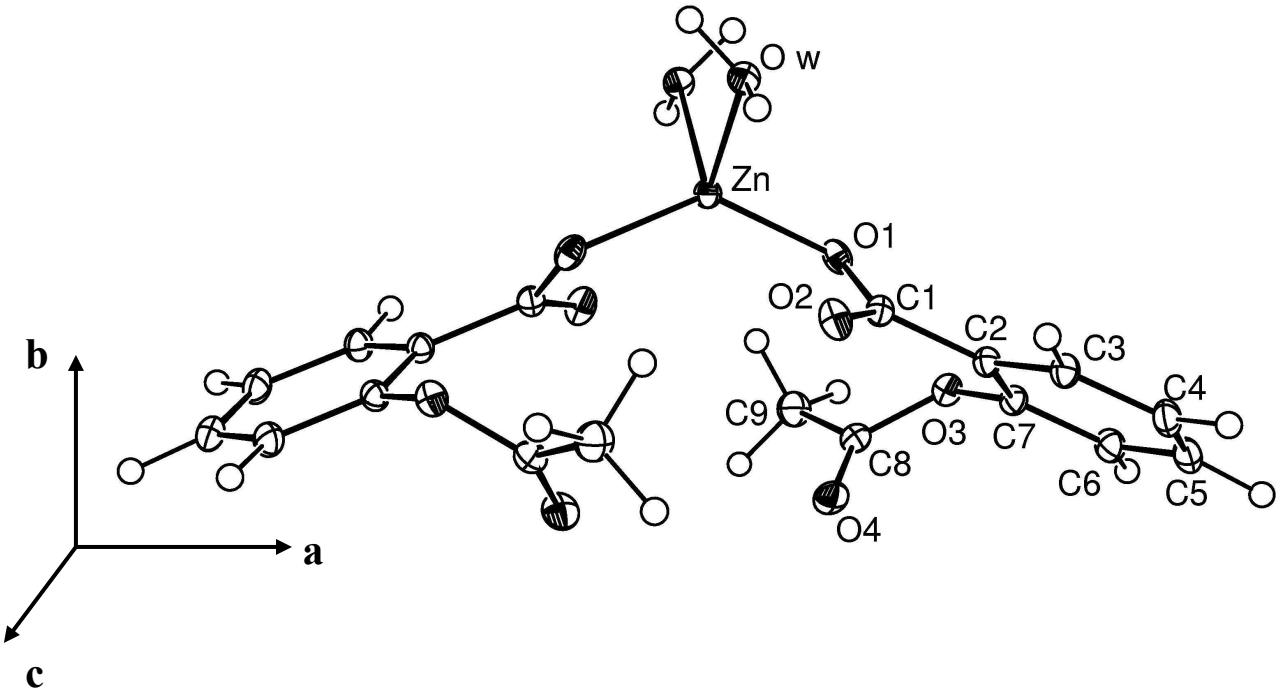

Figure 3a

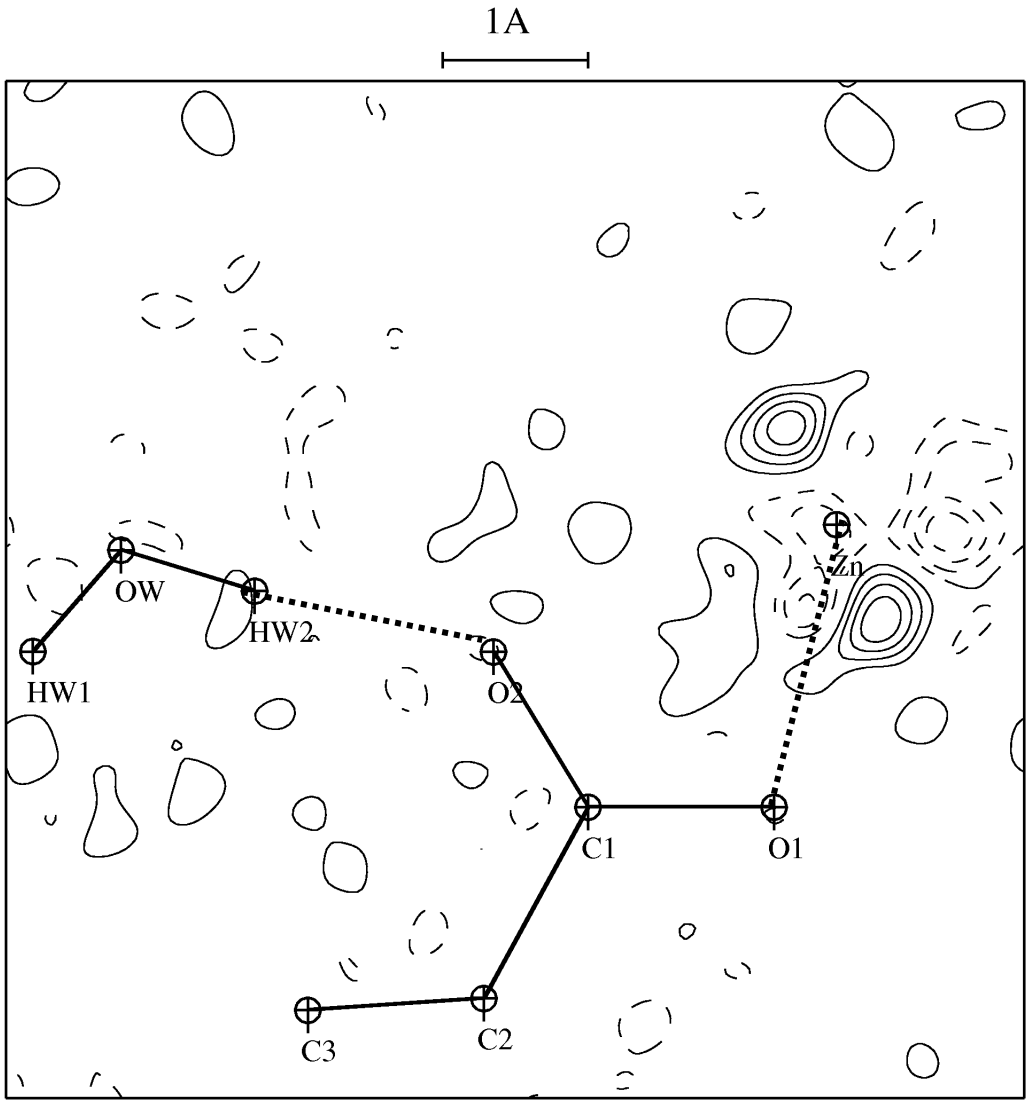

Figure 3b

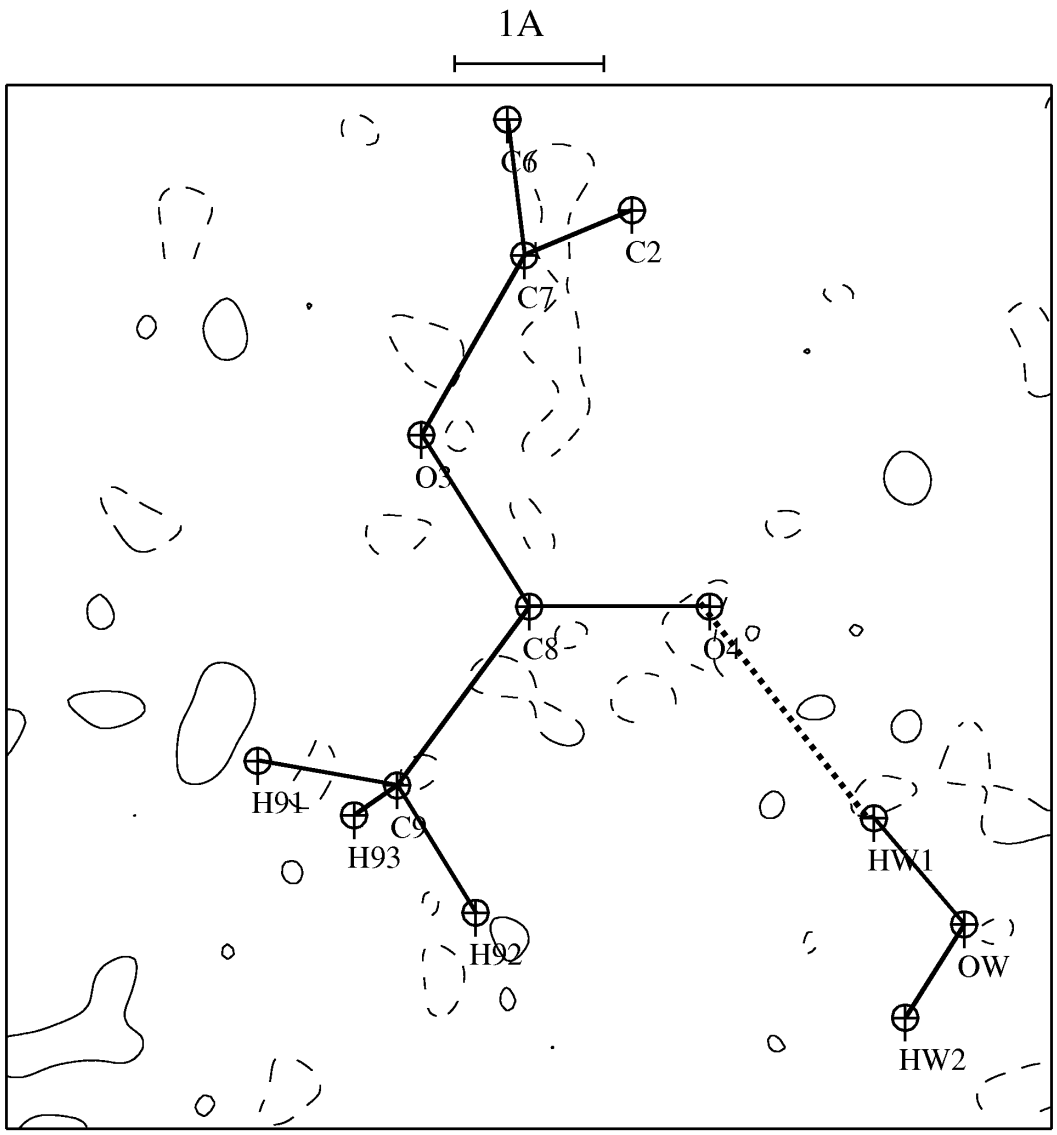

Figure 4a

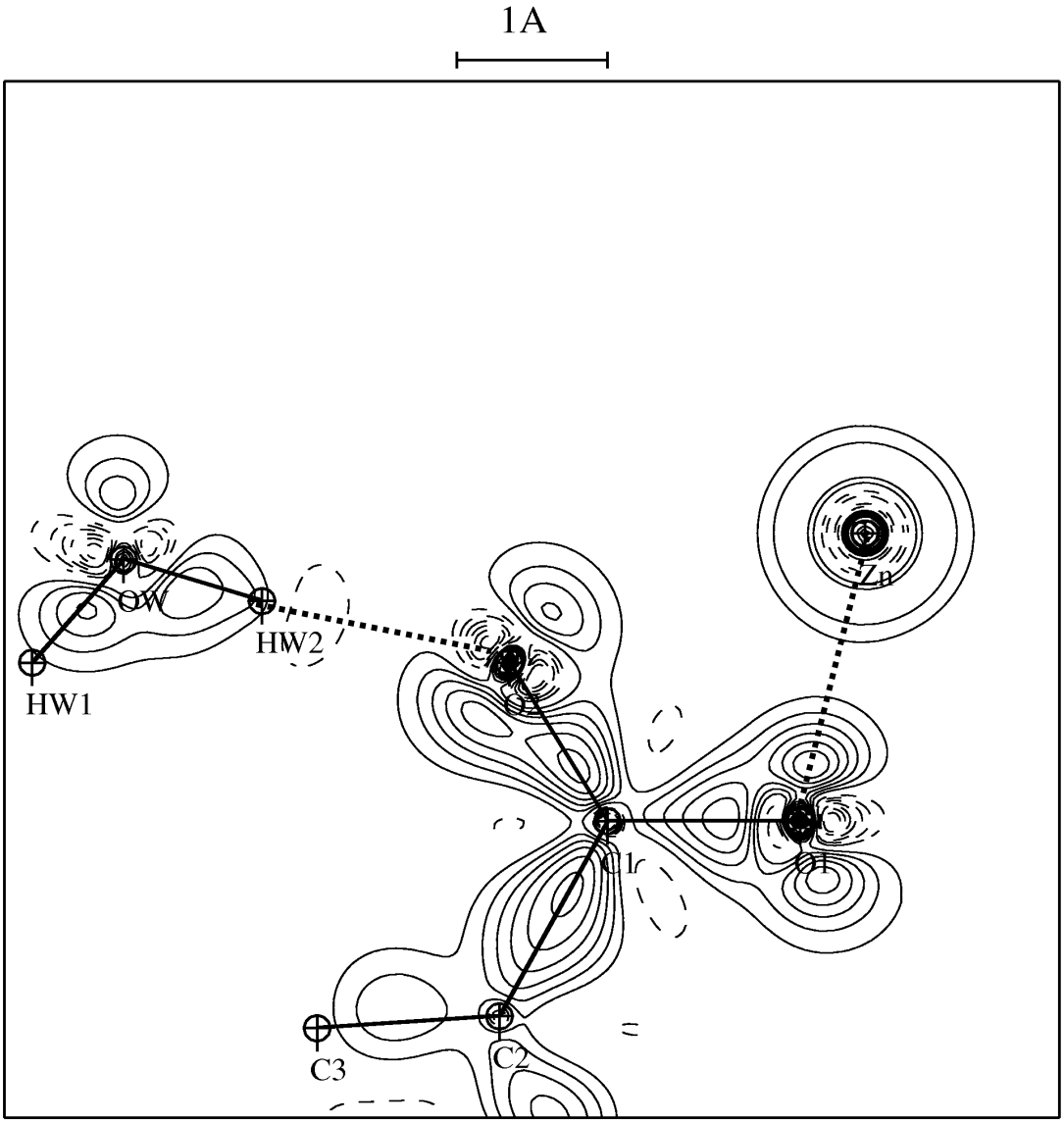

Figure 4b

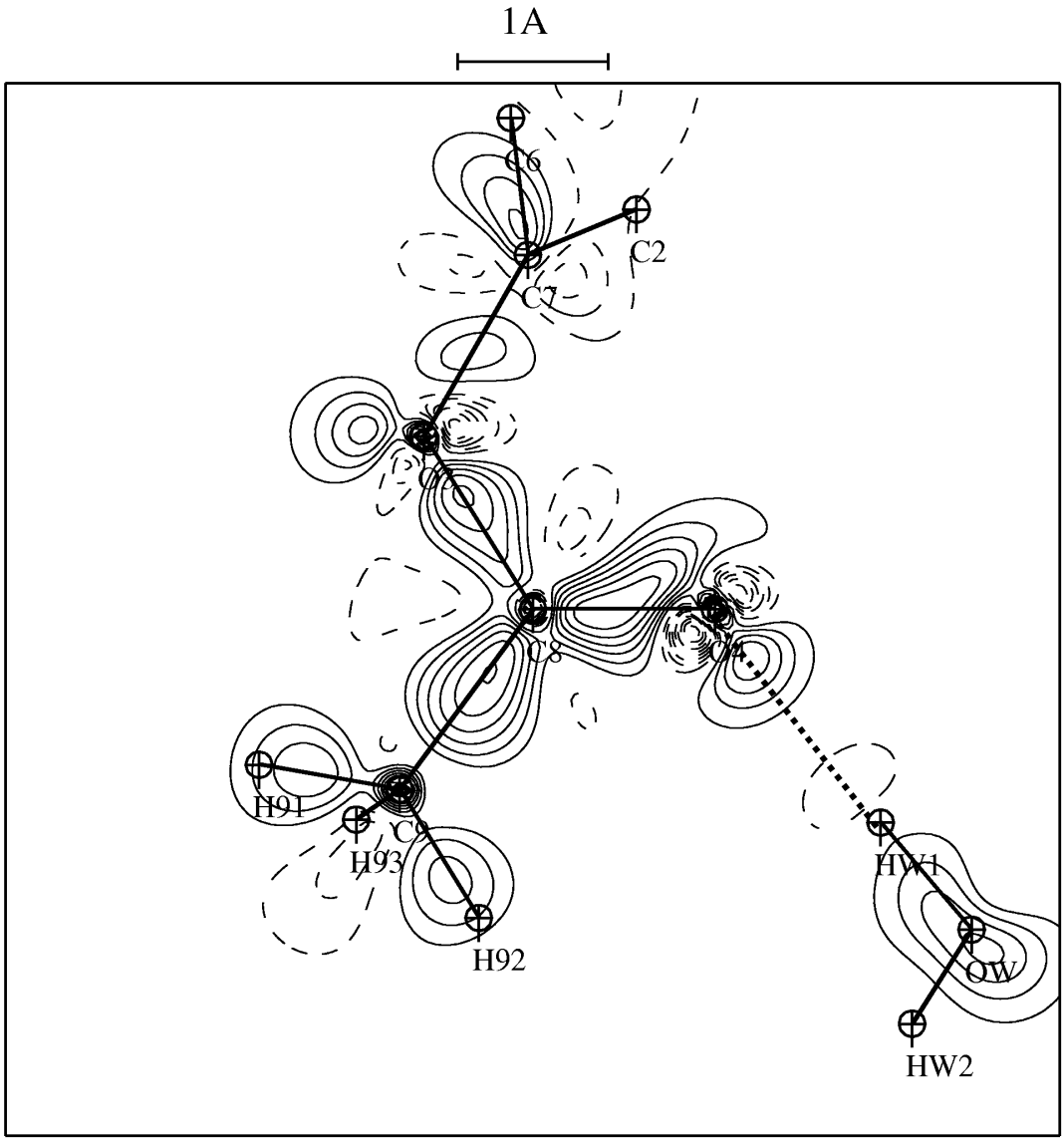

Figure 5

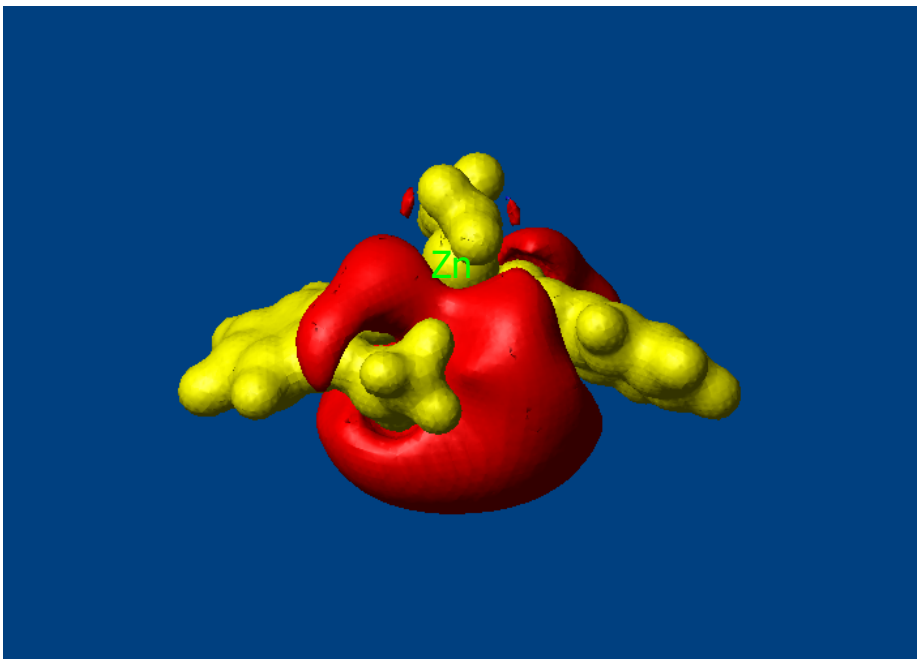

a

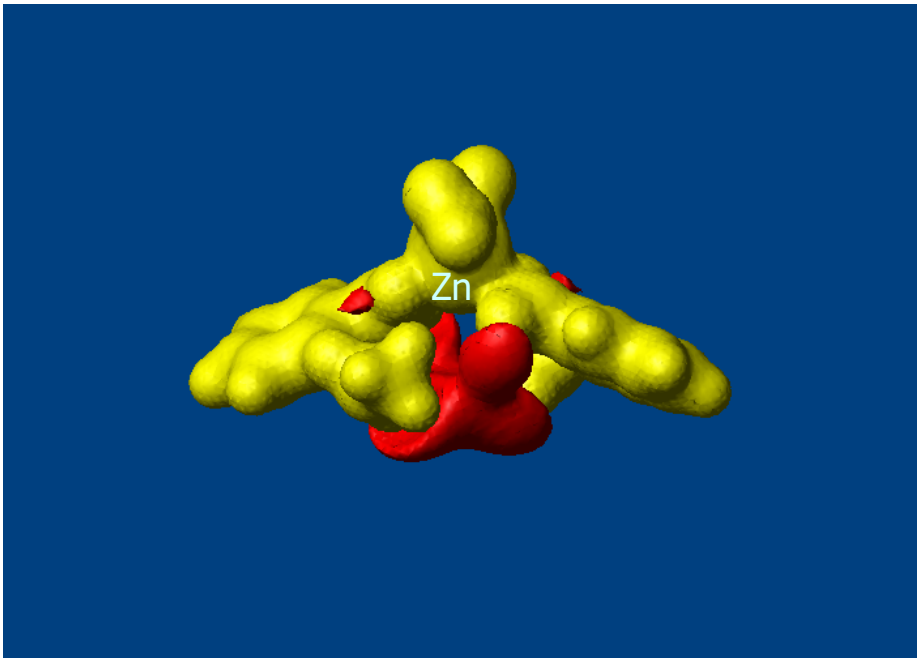

b

Figure 6

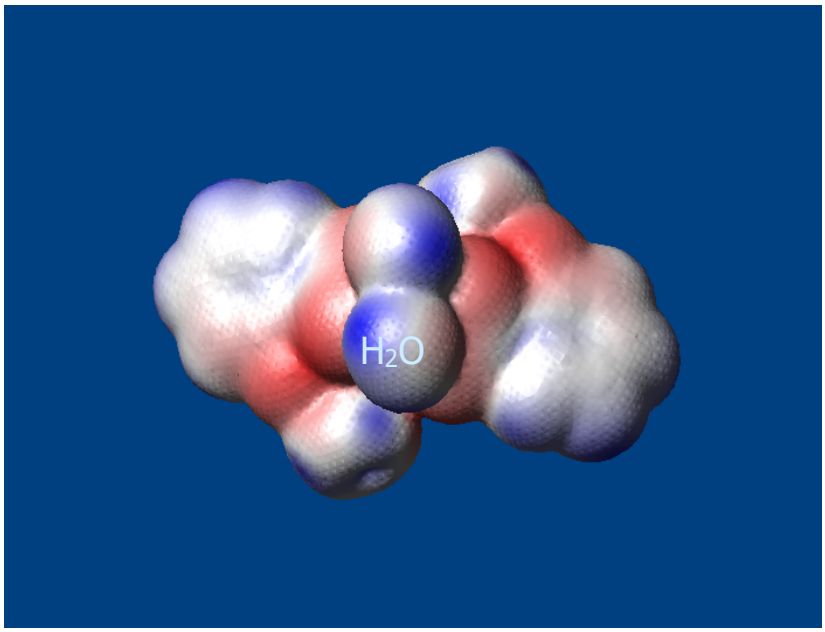

a

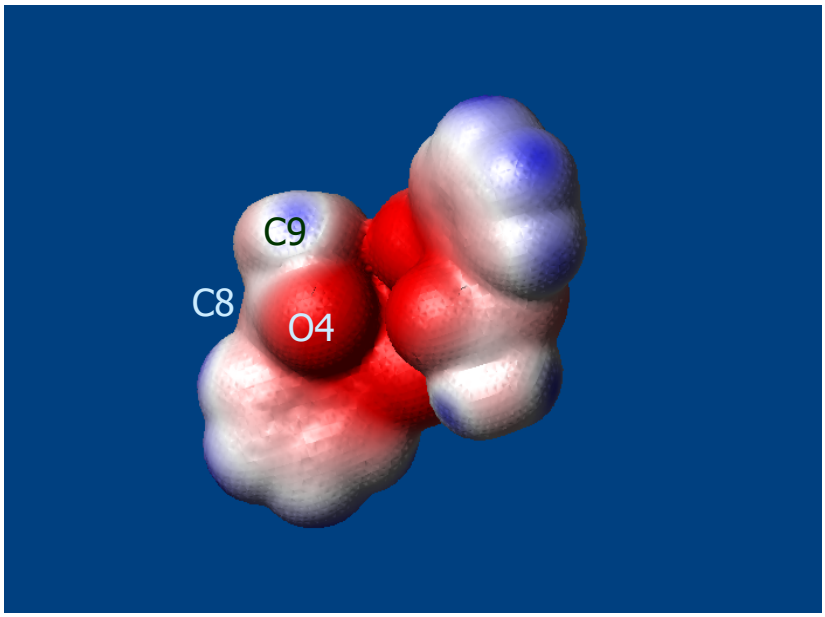

b

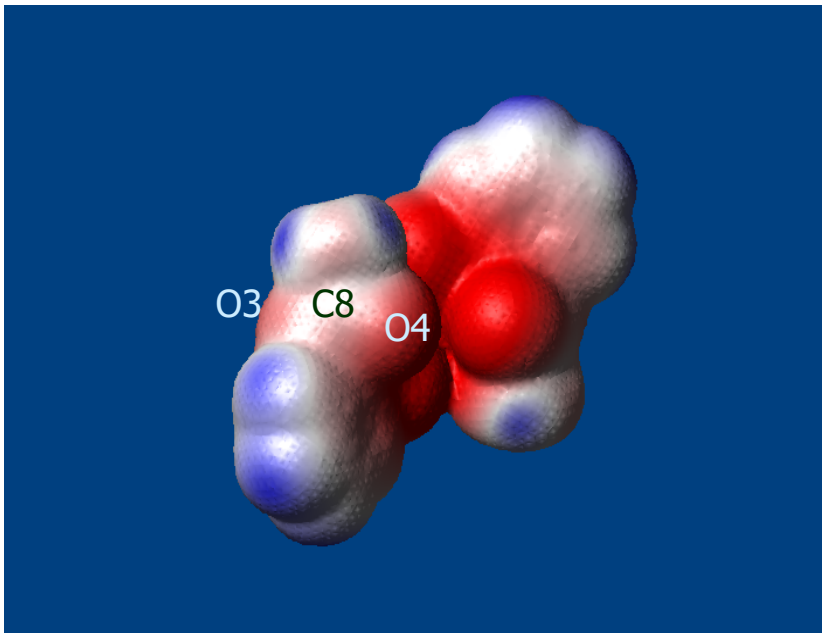

c